THE JOURNAL OF BIOLOGICAL CHEMISTRY
Vol. 273, No. 33, Issue of August 14, pp. 20758–20763, 1998
Printed in U.S.A.

Interaction of 2-*n*-Heptyl-4-Hydroxyquinoline-*N*-Oxide with Dimethyl Sulfoxide Reductase of *Escherichia coli**

(Received for publication, January 29, 1998, and in revised form, May 22, 1998)

Zhongwei Zhao and Joel H. Weiner‡

From the Department of Biochemistry and the Medical Research Council Group in the Molecular Biology of Membranes, University of Alberta, Edmonton, Alberta T6G 2H7, Canada

We have studied the interaction of the menaquinol analog 2-*n*-heptyl-4-hydroxyquinoline-*N*-oxide (HOQNO) with dimethyl sulfoxide reductase (DmsABC) and the effect of a mutation in the DmsC subunit (DmsABC^{H65R}) using fluorescence titration and stopped-flow methods. The titration data show that the HOQNO fluorescence is quenched when HOQNO binds to DmsABC. The binding stoichiometry is determined to be about 1:1. The mutant DmsABC^{H65R} blocks HOQNO binding to the protein. It is therefore proposed that there is one high-affinity HOQNO binding site per DmsABC molecule located in the DmsC subunit. Stopped-flow kinetic studies show that the interaction can be described by a two-step equilibrium model, a fast bimolecular step followed by a slow unimolecular step. The quenching of HOQNO fluorescence occurs in the bimolecular step. The rates for the forward and reverse reaction of the first equilibrium are determined to be $k_1 = (3.9 \pm 0.3) \times 10^5$ M^{-1} s^{-1} and $k_2 = 0.10 \pm 0.01$ s^{-1}, respectively. The dissociation constant for the first equilibrium, $K_{d1} = k_2/k_1$, is calculated to be about 260 nM. The upper limit of the overall dissociation constant is estimated to be 6 nM.

Escherichia coli is capable of growing anaerobically by inducing specialized respiratory chains that consist of a group of primary dehydrogenases, an intermediate electron carrier (menaquinone or ubiquinone), and a series of terminal reductases. Dimethyl sulfoxide reductase (DmsABC)[1] is one of the terminal reductases (1), and it catalyzes reduction of dimethyl sulfoxide and a variety of *S*- and *N*-oxides (2). This membrane-associated heterotrimer contains a catalytic subunit with a molybdenum cofactor (DmsA, 87.4 kDa), an electron-transfer subunit with four [4Fe-4S] clusters (DmsB, 23.1 kDa), and a membrane-intrinsic anchor subunit (DmsC, 30.8 kDa) (3).

DmsC is a hydrophobic polypeptide that traverses eight times and anchors the DmsAB dimer to the membrane (4). It is involved in menaquinol (MQH_2) binding and oxidation, and in electron transport. DmsABC is able to draw electrons from the menaquinol pool to DmsC and transfer them through DmsB to the catalytic subunit, DmsA. In a recent electron paramagnetic resonance (EPR) study (5), it was shown that DmsC^{H65} is involved in MQH_2 binding and oxidation. It was suggested that a mutation of the DmsC subunit, DmsC^{H65R}, may block binding of the MQH_2 analog HOQNO to the protein. However, there was no direct observation available about this possible blockage of HOQNO binding.

For another terminal reductase, fumarate reductase, it has been reported that there are two separate MQH_2 binding sites located in subunits C and D of the enzyme, respectively (6–8). The MQH_2 binding affinity of the site in subunit D is higher than that of the site in subunit C. For DmsABC, however, the number and the location of MQH_2 binding site(s) have not been determined.

HOQNO is a structural analog of MQH_2, and it is known as a classical inhibitor of the mitochondrial cytochrome *c* reductase. An earlier study showed that the fluorescence of HOQNO was completely quenched by binding to submitochondrial particles of beef heart (9). It was concluded that the inhibition of electron transfer by HOQNO was caused by binding to the specific binding site. Fluorescence quenching was also observed when an HOQNO analog, NQNO, bound to the mitochondrial cytochrome *c* reductase (10). NQNO is a specific inhibitor of the inner facing quinone-reaction center (Q_i) of the mitochondrial cytochrome *c* reductase. The fluorescence of HOQNO has provided a convenient means for studying HOQNO binding and inhibition reactions. It is expected, therefore, that a fluorescence spectroscopic study of the interaction of HOQNO with DmsABC could provide useful information for determining the number and the location of MQH_2 binding site(s) in DmsABC.

In this paper, we examine the binding stoichiometry and kinetics for the interaction of HOQNO with DmsABC using fluorescence titration and stopped-flow methods. We show that HOQNO binds to DmsABC with approximately 1:1 stoichiometry and the interaction can be described by a two-step equilibrium model. We also provide evidence that a mutation of the DmsC subunit, DmsABC^{H65R}, blocks the binding of the MQH_2 analog HOQNO to the protein as suggested recently in an EPR study (5).

EXPERIMENTAL PROCEDURES

Bacterial Strains and Plasmids—E. coli HB101 [*supE44 hsdS20 2(r_B^- m_B^-) recA13 ara-14 proA2 lacY1 galK2 rpsL20 xyl-5 mtl-1*] (11) was used for expression of wild-type and mutant DmsABC. For overexpression of DmsABC and DmsABC^{H65R}, bacteria were transformed with pDMS160 and pDMS160-H65R, respectively (5, 12, 13). All manipulations of strains were carried out as described by Sambrook *et al.* (14).

Growth of Cells and Preparation of Membrane Vesicles—Cells were grown anaerobically in 20-liter batches at 37 °C on a glycerol-fumarate minimal medium for 48 h as described previously (15). Cells were harvested using a Pellicon membrane system (16), washed, lysed by passage through a French pressure cell, and subjected to differential centrifugation. The isolated membranes were resuspended in 100 mM MOPS and 5 mM EDTA (pH 7.0), frozen in liquid nitrogen, and then stored at −70 °C until use (12). Protein concentrations were determined

* This work was funded by Grant PG-11440 from the Medical Research Council of Canada (to J. H. W.). The costs of publication of this article were defrayed in part by the payment of page charges. This article must therefore be hereby marked "*advertisement*" in accordance with 18 U.S.C. Section 1734 solely to indicate this fact.

‡ To whom correspondence should be addressed. Tel.: 403-492-2761; Fax: 403-492-0886; E-mail: joel.weiner@ualberta.ca.

[1] The abbreviations used are: DmsABC, dimethyl sulfoxide reductase; HOQNO, 2-*n*-heptyl-4-hydroxyquinoline-*N*-oxide; NQNO, 2-*n*-nonyl-4-hydroxyquinoline-*N*-oxide; MQH_2, menaquinol; EPR, electron paramagnetic resonance; MOPS, 3-(*N*-morpholino)propanesulfonic acid.

by a modified Lowry assay in the presence of 1% SDS using a Bio-Rad serum albumin protein standard (17). The concentration of DmsABC was calculated from the total concentration of [4Fe-4S] clusters measured by the EPR spin quantitation and by assuming that there are four [4Fe-4S] clusters per DmsABC molecule (18, 19).

Quenching of HOQNO Fluorescence by Binding to DmsABC—HOQNO was obtained from Sigma. The concentration of HOQNO was determined spectrophotometrically after diluting the ethanolic stock solution in 1 mM sodium hydroxide using an extinction coefficient of 9450 M^{-1} cm^{-1} at 346 nm (20). Fluorescence measurements were carried out using a Perkin-Elmer LS-50B luminescence spectrometer. The fluorescence emission spectrum of HOQNO in 100 mM MOPS and 5 mM EDTA (pH 7.0) exhibits a maximum at 479 nm with the excitation at 341 nm (data not shown). In fluorescence titration experiments, aliquots of a 50 μM HOQNO stock solution were added to the cuvette containing the protein in 100 mM MOPS and 5 mM EDTA (pH 7.0), and fluorescence emissions were measured at 479 nm (with excitation at 341 nm). The background fluorescence of the protein sample in the absence of HOQNO was subtracted from the fluorescence of the sample in the presence of HOQNO.

Stopped-flow Experiment and Data Analysis—The stopped-flow experiments were performed using a Sequential Bio SX-17MV stopped-flow spectrofluorimeter (Applied Photophysics Ltd., Leatherhead, UK). In a typical experiment, DmsABC or DmsABC^{H65R} (1 or 2 μM) in 100 mM MOPS and 5 mM EDTA (pH 7.0) was mixed with an equal volume of various concentrations of HOQNO (1–14 μM) in the same buffer. Temperature was maintained at 25 °C. The fluorescence of HOQNO was excited at 341 nm, and the emissions above 400 nm were recorded through a cut off filter SGG-400-1.00 (CVI Laser Co., Albuquerque, NM). For each concentration of HOQNO, at least three runs were performed and 1000 or 2000 data points were collected. After averaging, data were fitted to an appropriate equation using the software supplied by Applied Photophysics. Under our experimental conditions, quenching of HOQNO fluorescence by binding to DmsABC was biphasic, and the observed fluorescence, F, was best fitted to a double exponential equation,

$$F = A_f e^{-k_f t} + A_s e^{-k_s t} + b \quad \text{(Eq. 1)}$$

where A_f and A_s are the amplitudes of the fast and slow phase, and k_f and k_s are the observed rates for the fast and slow phase, respectively, t is time and b is an off set value of the stopped-flow instrument.

The interaction of HOQNO with DmsABC can be described by the following model (21–23) (see "Discussion"),

$$E + L \underset{k_2}{\overset{k_1}{\rightleftharpoons}} EL \underset{k_4}{\overset{k_3}{\rightleftharpoons}} EL^* \quad \text{(Eq. 2)}$$

where E represents DmsABC; L, the ligand (HOQNO); EL, the initial complex of DmsABC with HOQNO before the isomerization takes place; EL^*, the final complex product; k_1 and k_3 are the rate constants for the forward reactions in M^{-1} s^{-1} and s^{-1}, respectively, and k_2 and k_4 are the rate constants for the reverse reactions in s^{-1}. In the case where the bimolecular process is much faster than the unimolecular process and the initial concentration of L is much higher than the concentration of E, the observed first-order rates for the fast phase (k_f) and the slow phase (k_s) are given by Equations 3 and 4, respectively,

$$k_f = k_2 + k_1[L] \quad \text{(Eq. 3)}$$

$$k_s = k_4 + k_3/\{1 + K_{d1}/[L]\} \quad \text{(Eq. 4)}$$

where $K_{d1} = k_2/k_1$ is the dissociation constant of the first equilibrium in Equation 2.

Under our experimental conditions, the plot of HOQNO fluorescence against the concentration of HOQNO was linear up to 7 μM of HOQNO (after mixing) (data not shown). This was, therefore, the highest concentration of HOQNO used in this work. Toward the low end of the HOQNO concentrations used herein, the condition that initial concentration of L is much higher than the concentration of E (0.5 μM after mixing) does not hold. However, the observed first-order rates for the fast phase, k_f, can still be analyzed using Equation 3 as demonstrated by Halford (21).

From the fit of the observed k_f data to Equation 3, k_1 and k_2 can be obtained. Under our experimental conditions, deviations of the observed k_s were too large to be fitted to Equation 4 to yield reliable k_3 and k_4. To evaluate the values of k_3 and k_4, another approach using the Glint program (Applied Photophysics) was employed. This program enables one to globally analyze a complete data set measured at all wavelengths according to a proposed reaction scheme and to obtain the reaction parameters from the best fit of the calculated data to the experimental data. Kinetic data irrelevant of wavelength (the case of this work) or measured at a single wavelength can also be analyzed using this program. In this work, using the reaction scheme (Equation 2), and the k_1 and k_2 determined from Equation 3, kinetic traces measured at various HOQNO concentrations were analyzed using the Glint program, and the values of k_3 and k_4 were evaluated from the good fits of the calculated kinetic traces to the observed traces.

RESULTS

Stoichiometry of HOQNO Binding to DmsABC—The binding of HOQNO to DmsABC was examined by measuring the HOQNO fluorescence emission (at 479 nm with excitation at 341 nm) in the absence and in the presence of DmsABC. In the absence of DmsABC, the plot of fluorescence measured by titrating the buffer (100 mM MOPS and 5 mM EDTA, pH 7.0) against the concentration of HOQNO gave a straight line with a positive slope as shown in Fig. 1*A*. This fluorescence was attributed to free HOQNO molecules (not bound to other compounds). In the presence of DmsABC, however, the initial portion of each titration curve was flat (Fig. 1*A*), indicating that there was no increase of fluorescence intensity upon the addition of a certain concentration of HOQNO to the protein. In other words, there was no free HOQNO present in the system to emit fluorescence. It was clear that the fluorescence of HOQNO was quenched in the presence of DmsABC and this quenching was because of HOQNO binding to DmsABC. Further addition of HOQNO to the protein caused a sudden increase of fluorescence intensity, suggesting that free HOQNO became available when the amount of HOQNO added to the protein was higher than a certain concentration at a given concentration of DmsABC.

It was not possible to construct a Scatchard plot from the titration data in Fig. 1*A* because of the sharp transition of the titration curves. To obtain the stoichiometry of HOQNO binding to DmsABC, four concentrations of DmsABC (0.25, 0.5, 0.75, and 1.0 μM) were titrated with HOQNO in 100 mM MOPS and 5 mM EDTA at pH 7.0 (Fig. 1*A*). The extrapolations of the linear portions of the titration curves to zero fluorescence yield four intercepts on the x-axis of the plot. These intercepts represent the concentrations of HOQNO bound to DmsABC at the given concentrations of DmsABC. Therefore, from the plot of the intercepts against the concentration of DmsABC, Fig. 1*B*, the stoichiometry of HOQNO binding to DmsABC can be determined to be approximately 1:1.

Effect of DmsABC^{H65R} Mutation on HOQNO Binding to the Protein—It has been suggested in a recent EPR study (5) that residue His-65 in the DmsC subunit may be involved in MQH_2 binding and a His to Arg mutation, DmsABC^{H65R}, may block binding the MQH_2 analog HOQNO to the protein. To verify this, titrations of 0.4 μM wild-type DmsABC and mutant DmsABC^{H65R} with HOQNO in 100 mM MOPS and 5 mM EDTA (pH 7.0) were carried out and the data obtained were compared as shown in Fig. 2. For the wild-type protein, the initial portion of the titration curve was flat indicating quenching of HOQNO fluorescence because of HOQNO binding to the protein. Further increase of HOQNO concentration caused a sharp increase of fluorescence intensity. For the mutant DmsABC^{H65R}, however, the titration data gave a straight line with a positive slope, indicating that there was no quenching of HOQNO fluorescence. In other words, in the case of titration of DmsABC^{H65R}, the HOQNO added to the protein was in the free form and not bound to the protein. Fig. 2, thus, demonstrates that the mutation of DmsABC^{H65R} blocks HOQNO binding to the protein.

Stopped-flow Studies of Interaction of HOQNO with DmsABC—To investigate the kinetics and mechanism of the

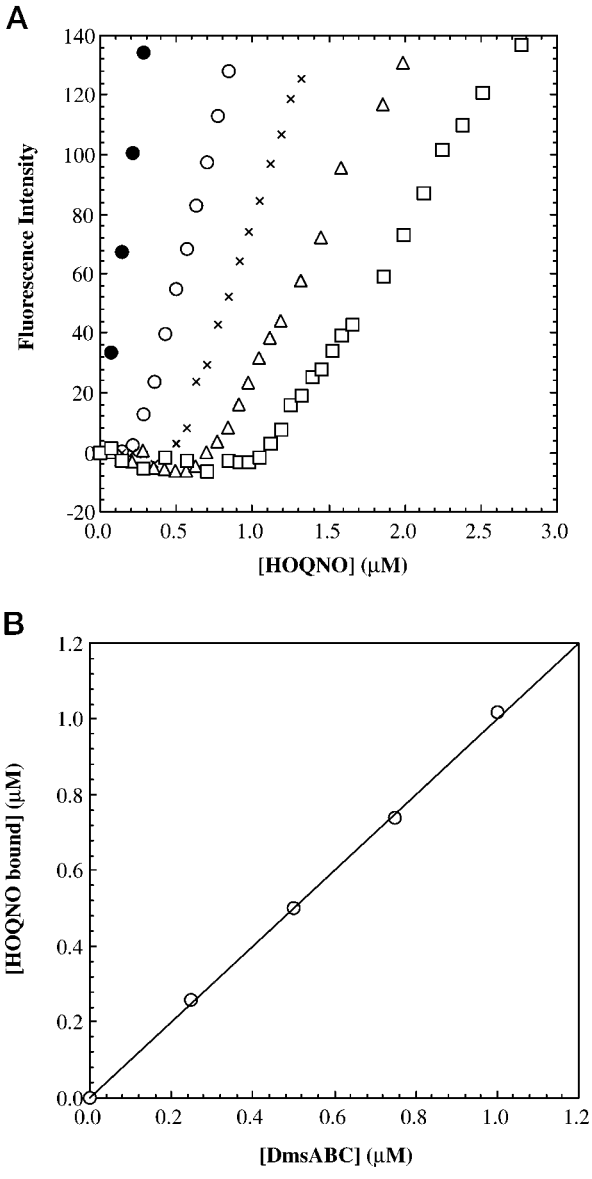

FIG. 1. **Determination of the stoichiometry of HOQNO binding to DmsABC.** *Panel A,* titrations of the buffer of 100 mM MOPS and 5 mM EDTA (pH 7.0) ( ), and 0.25 (○), 0.5 (×), 0.75 (Δ), and 1.0 (□) μM DmsABC in the same buffer with HOQNO. Fluorescence emission data at 479 nm (with excitation at 341 nm) were obtained by subtracting the background fluorescence of the protein. *Panel B,* plot of the concentration of HOQNO bound to DmsABC against the concentration of the protein. The concentrations of HOQNO bound to DmsABC were determined by extrapolating the linear portions of the titration curves in *panel A* to zero fluorescence.

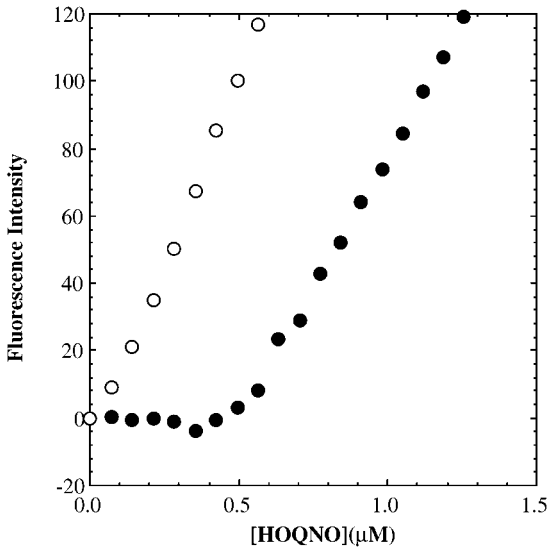

FIG. 2. **Comparison of fluorescence titration data for wild-type DmsABC and the mutant DmsABC^{H65R}.** 0.4 μM wild-type DmsABC ( ) and mutant DmsABC^{H65R} (○) were titrated with HOQNO in 100 mM MOPS and 5 mM EDTA (pH 7.0). Fluorescence emission data at 479 nm (with excitation at 341 nm) were obtained by subtracting the background fluorescence of the protein solution.

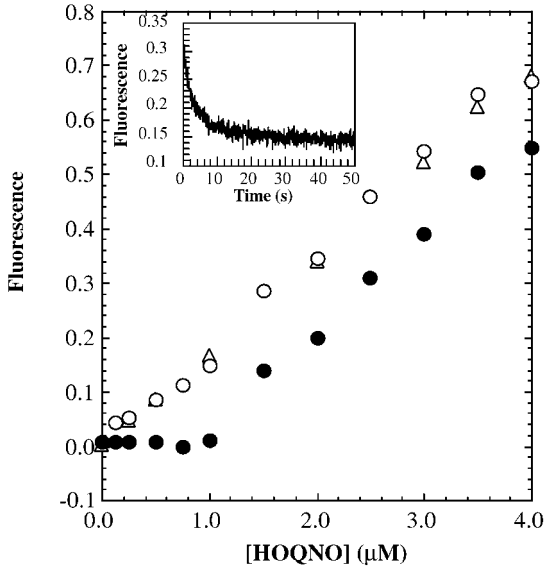

FIG. 3. **Fluorescence quenching observed by mixing HOQNO with wild-type DmsABC using the stopped-flow method.** A variety of concentrations of HOQNO in the buffer of 100 mM MOPS and 5 mM EDTA at pH 7.0 were rapidly mixed with the same buffer (Δ) or mixed with 2 μM DmsABC in the same buffer, (○) and ( ). At a given concentration of HOQNO, fluorescence quenching was observed from the decrease of the initial fluorescence intensity (○) (measured immediately after mixing) to the final fluorescence intensity ( ) (measured 50 s after mixing). The *inset* shows the decrease of fluorescence intensity with time observed after mixing 2 μM DmsABC with 3 μM HOQNO.

interaction of HOQNO with DmsABC, the stopped-flow fast kinetic technique was employed. Fig. 3 shows a plot of the observed fluorescence intensities against the concentration of HOQNO obtained by mixing various concentrations of HOQNO in buffer of 100 mM MOPS and 5 mM EDTA (pH 7.0) with the same buffer or with 2 μM wild-type DmsABC (in the buffer). After mixing the protein with HOQNO, a decrease of fluorescence intensity with time was observed as shown in the inset of Fig. 3 indicating quenching of HOQNO fluorescence. The magnitude of the initial fluorescence intensity measured immediately after mixing HOQNO with DmsABC was very similar to the magnitude of the fluorescence intensity measured in the absence of the protein, indicating that no detectable reaction occurred during the dead time of the stopped-flow instrument. The same results were also obtained by mixing 1 μM of DmsABC with various concentrations of HOQNO in 100 mM MOPS and 5 mM EDTA (pH 7.0) under the conditions in Figs. 5*B* and 6 (data not shown). On the other hand, for the final fluorescence intensity measured 50 s after mixing, the initial portion of the curve was flat and the intercept on the *x*-axis (about 1 μM) obtained by extrapolating the linear portion of the curve to zero fluorescence was in good agreement with the 1:1 binding stoichiometry obtained under the steady-state conditions (Figs. 1 and 2). Fig. 3 demonstrates that the fluorescence quenching observed after mixing HOQNO with DmsABC is because of HOQNO binding to the protein.

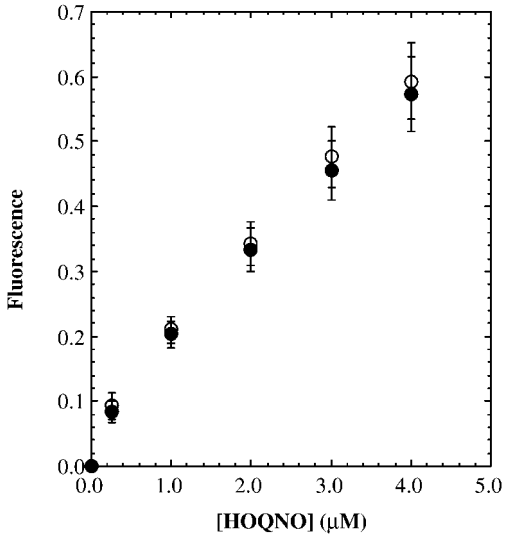

FIG. 4. **Fluorescence observed by mixing DmsABC^{H65R} with HOQNO using the stopped-flow method.** 2 μM of DmsABC^{H65R} was rapidly mixed with various concentrations of HOQNO in 100 mM MOPS and 5 mM EDTA at pH 7.0. ○, the initial fluorescence intensity measured immediately after mixing; , the final fluorescence intensity measured 50 s after mixing.

The DmsABC^{H65R} mutant was used as a non-HOQNO binding control for this work. Fig. 4 shows the plot of the fluorescence intensities against the concentration of HOQNO obtained by mixing 2 μM mutant DmsABC^{H65R} with various concentrations of HOQNO in 100 mM MOPS and 5 mM EDTA (pH 7.0). In contrast to Fig. 3, the plot of the initial fluorescence intensity (measured immediately after mixing) and the final fluorescence intensity (measured 50 s after mixing) against the concentration of HOQNO gave two straight lines that not only had the same slope but also overlapped each other within experimental error. Clearly, there was no significant quenching of HOQNO fluorescence in this case. Fig. 4 indicates that the mutation of DmsABC^{H65R} blocks HOQNO binding to the protein, which agrees with the steady-state titration data (Fig. 2). Furthermore, this result serves as a good control for the stopped-flow experiment, confirming that the nonlinear feature of the curve for the final fluorescence intensity in Fig. 3 is not because of an artifact.

As shown in Fig. 3, binding HOQNO to DmsABC causes a quenching of HOQNO fluorescence, and this quenching process can be followed using the stopped-flow method. To further investigate the kinetics of HOQNO binding to DmsABC, 1 μM DmsABC was rapidly mixed with various concentrations of HOQNO using the stopped-flow method. Fig. 5*A* shows a typical trace of fluorescence quenching observed after mixing 1 μM of DmsABC with 2 μM HOQNO in 100 mM MOPS and 5 mM EDTA at pH 7.0 (25 °C) and the residuals for fitting these data to Equation 1. The fluorescence quenching process was completed about 50 s after mixing. The observed quenching trace had two phases, a fast phase followed by a slow phase, and it was best fitted with the double exponential equation, Equation 1. This was also true at other HOQNO concentrations used in this work (Fig. 5*B*). From the fit, the observed first-order rates and the amplitudes for the fast and slow phase at the given concentration of HOQNO, k_f, k_s, A_f, and A_s, can be determined. The first-order rate for the fast phase (k_f) observed by mixing 1 μM DmsABC with various concentrations of HOQNO in 100 mM MOPS and 5 mM EDTA at pH 7.0 (25 °C) was plotted against the concentration of HOQNO and the data obtained were fitted to Equation 3 as shown in Fig. 5*B*, from which the rate constants for the forward and reverse reactions of the first equilibrium in Equation 2 were determined to be $k_1 = (3.9 \pm 0.3) \times 10^5$ M^{-1} s^{-1} and $k_2 = 0.10 \pm 0.01$ s^{-1} respectively. Thus the dissociation constant for the first equilibrium, $K_{d1} = k_2/k_1$, was calculated to be about 260 nM.

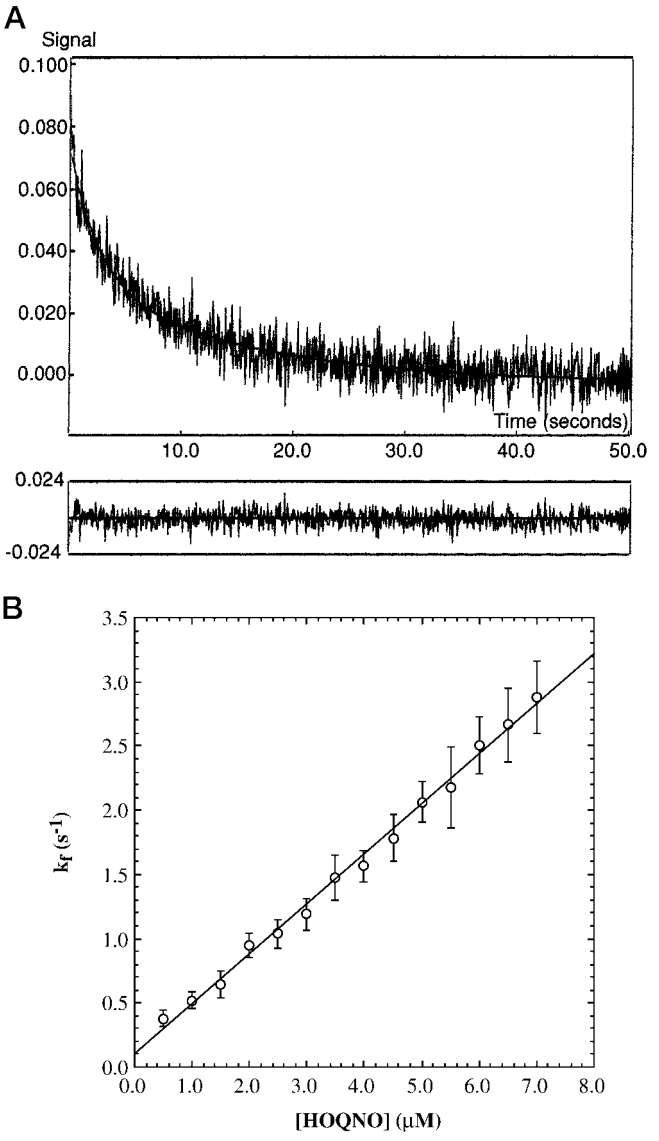

FIG. 5. **Kinetic analysis of fluorescence quenching because of the interaction of HOQNO with DmsABC.** *A*, quenching of HOQNO fluorescence observed by mixing 1 μM of DmsABC with 2 μM HOQNO in 100 mM MOPS and 5 mM EDTA at pH 7.0 (25 °C) and the fit of these data to Equation 1. From the fit, the observed first-order rates and the amplitudes for the fast and slow phase were determined to be $k_f = 0.52 \pm 0.06$ s^{-1}, $k_s = 0.07 \pm 0.008$ s^{-1}, $A_f = 0.041 \pm 0.003$, and $A_s = 0.035 \pm 0.003$, respectively. The *lower part* of the figure shows the residuals of the fit. *B*, effect of HOQNO concentration on k_f. The k_f data were determined in the same way as described in *panel A*, except varying HOQNO concentrations. The *solid line* represents the fit of the k_f data to Equation 3, from which the rate constants for the first equilibrium in Equation 2 were determined to be $k_1 = (3.9 \pm 0.3) \times 10^5$ M^{-1} s^{-1} and $k_2 = 0.10 \pm 0.01$ s^{-1}, respectively.

The rate constants for the forward and reverse reactions of the second equilibrium in Equation 2, k_3 and k_4, were evaluated with the Glint program (Applied Photophysics). Using the reaction scheme described in Equation 2, and the k_1 ($=3.9 \times 10^5$ M^{-1} s^{-1}) and k_2 ($= 0.10$ s^{-1}) determined from the fit as shown in Fig. 5*B*, $k_3 = 0.40 \pm 0.04$ s^{-1} and $k_4 \leq 0.01$ s^{-1} were obtained from the good fits of the calculated kinetic traces to the observed traces (data not shown). Therefore, the association constant of the second equilibrium, $K_{a2} = k_3/k_4 \geq 40$, was

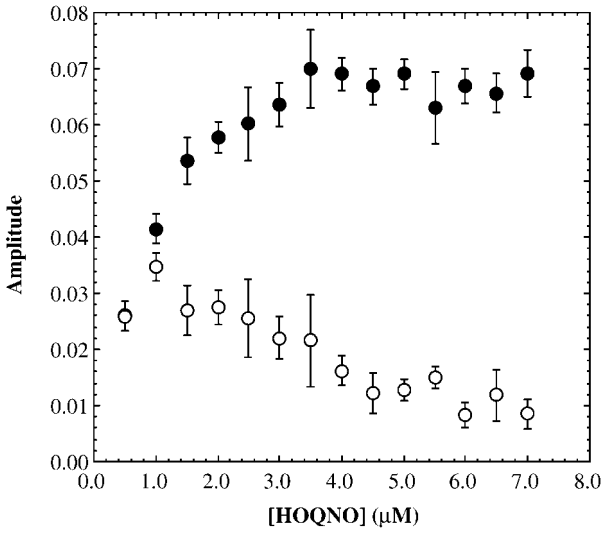

FIG. 6. **Dependence of A_f and A_s on HOQNO concentration.** The amplitudes for the fast phase A_f (●) and slow phase A_s (○) were obtained by mixing 1 μM of DmsABC with various concentrations of HOQNO in 100 mM MOPS and 5 mM EDTA at pH 7.0 (25 °C) and by fitting the observed traces to Equation 1.

obtained. The upper limit of the overall dissociation constant for Equation 2 was thus estimated to be about 6 nM, *i.e.* $K_d^{overall} = K_{d1}/(1 + K_{a2}) \leq 6$ nM.

To investigate the effect of the ligand (HOQNO) concentration on the kinetics of HOQNO binding to DmsABC, the amplitudes for the fast phase (A_f) and the slow phase (A_s) were plotted against the concentration of HOQNO (Fig. 6). The A_f and A_s were obtained by mixing 1 μM DmsABC with various concentrations of HOQNO in 100 mM MOPS and 5 mM EDTA at pH 7.0 (25 °C) and by fitting the observed traces with Equation 1. The amplitude for the fast phase increased with the increase of HOQNO concentration up to about 4 μM then became saturated, whereas the amplitude for the slow phase increased initially with HOQNO concentration up to 1 μM and then it started to decrease with the increase of HOQNO concentration.

DISCUSSION

In bacterial anaerobic electron transport menaquinol shuttles reducing equivalents from the primary dehydrogenases to the terminal reductases within the cytoplasmic membrane. However, relatively little is known about the interaction of menaquinol with these enzymes. In this study, we have utilized direct steady state and rapid reaction methodologies to investigate the binding of a fluorescent analog of menaquinol to DmsABC. We have shown that HOQNO interacts with very high affinity and 1:1 stoichiometry at a site within the DmsC subunit. Mutation of His-65 to Arg in DmsC blocks quinol activity and eliminates HOQNO binding. Our finding of only one exchangeable binding site, by direct measurement, differs from studies with fumarate reductase (6–8) and nitrate reductase (24), where two quinol binding sites have been proposed by indirect methods.

In the stopped-flow studies, the biphasic nature of the observed quenching process and the nonlinear increase of the observed slow rate (k_s) with HOQNO concentration reaching a plateau at higher concentrations of HOQNO (data not shown) suggest that the two-step mechanism (Equation 2) (21–23), a fast bimolecular process followed by a slow unimolecular process, can be applied to describe the quenching process resulting from binding HOQNO to DmsABC. In this mechanism, it is assumed that a loosely bound complex of the HOQNO (L) with DmsABC (E), EL, is formed rapidly by a bimolecular association and then it is converted to a more tightly and specifically bound complex, EL^*, by a slow unimolecular process (isomerization). The isomerization may take place through several possible pathways, such as rearrangement of EL without any conformational change in E or L, a conformational change in either E or L, or conformational changes in both E and L (22).

It is expected that stopped-flow kinetic studies can provide some useful information about the bimolecular association of HOQNO with DmsABC and the subsequent isomerization process. The effect of HOQNO concentration on the amplitudes of the fast and slow phase may be interpreted as follows. When the concentration of HOQNO is lower than or comparable with the dissociation constant of the first equilibrium in Equation 2, K_{d1}, but higher than the overall dissociation constant, only a small amount of protein is associated with the ligand (HOQNO) to form the complex EL by the fast bimolecular process, which is observed as a fast phase of quenching. The subsequent slow isomerization process of converting EL to EL^* would shift the first equilibrium in Equation 2 to the right-hand side slowly. This slow shift of the first equilibrium is observed as a subsequent slow phase of quenching. Alternatively, when the concentration of HOQNO is increased to higher than K_{d1}, more and more DmsABC molecules are associated with HOQNO to give EL through the fast bimolecular process, thus, less and less free DmsABC molecules are available for the subsequent shift of the first equilibrium to the right-hand side caused by the slow isomerization process. Therefore, the amplitude of the observed fast phase of quenching increases with increase of HOQNO concentration until becoming saturated, whereas the observed slow phase of quenching decreases with increase of HOQNO concentration, and this would finally result in that the amplitude of the slow phase would be negligible compared with the amplitude of the fast phase. These results suggest that the quenching of HOQNO fluorescence occurs in the bimolecular step of the association of E with L rather than in the unimolecular step of forming EL^* (see Equation 2).

Primary dehydrogenases and terminal reductases have been the subject of a large number of steady-state kinetic investigations (see Refs. 24–31 as examples), but rapid reaction methodologies have been limited because of the lack of available probes. We have now shown that fluorescent HOQNO can be used to monitor the quinol binding reaction. Although the steady-state methodology is useful for stoichiometry, the affinity is so tight that Scatchard plots are not useful. The stopped-flow method allows determination of rates and dissociation constants. Although the three-dimensional structures of several quinone-binding proteins have been determined (32, 33), it is not yet possible to define a quinone binding motif. This technique will prove useful in examining site-directed mutations in the quinol binding region or in conformationally coupled changes that alter quinone binding.

This work and a recent study on the interaction of HOQNO with fumarate reductase using EPR and steady-state fluorescence spectroscopic methods (34) demonstrate the utility of the characteristics of HOQNO fluorescence and its structural analogy to MQH_2 for studying interactions of MQH_2 with terminal reductases in respiratory chains. Studies on the interactions of HOQNO with *E. coli*. nitrate reductase[2] and with fumarate reductase[3] are in progress.

Acknowledgments—We thank Dr. R. A. Rothery for helpful discussions, assisting in protein preparations, and critically reading the manuscript, and Dr. H. B. Dunford in the Department of Chemistry, University of Alberta for providing the stopped-flow facility.

[2] R. A. Rothery, F. Blasco, and J. H. Weiner, unpublished results.
[3] Z. Zhao, R. A. Rothery, and J. H. Weiner, unpublished results.

REFERENCES

1. Weiner, J. H., Rothery, R. A., Sambasivarao, D., and Trieber, C. A. (1992) *Biochim. Biophys. Acta* **1102,** 1–18
2. Simala-Grant, J. L., and Weiner, J. H. (1996) *Microbiology* **142,** 3231–3239
3. Bilous, P. T., Cole, S. T., Anderson, W. F., and Weiner, J. H. (1988) *Mol. Microbiol.* **2,** 785–795
4. Weiner, J. H., Shaw, G., Turner, R. J., and Trieber, C. A. (1993) *J. Biol. Chem.* **268,** 3238–3244
5. Rothery, R. A., and Weiner, J. H. (1996) *Biochemistry* **35,** 3247–3257
6. Westenberg, D. J., Gunsalus, R. P., Ackrell, B. A. C., and Cecchini, G. (1990) *J. Biol. Chem.* **256,** 19560–19567
7. Westenberg, D. J., Gunsalus, R. P., Ackrell, B. A. C., Sices, H., and Cecchini, G. (1993) *J. Biol. Chem.* **268,** 815–822
8. Cecchini, G., Sices, H., Schroder, I., and Gunsalus, R. P. (1995) *J. Bacteriol.* **177,** 4587–4592
9. van Ark, G., and Berden, J. A. (1977) *Biochim. Biophys. Acta* **459,** 119–137
10. Brandt, U., and von Jagow, G. (1991) *Eur. J. Biochem.* **195,** 163–170
11. Boyer, H. W., and Roulland-Dussoix, D. (1969) *J. Mol. Biol.* **41,** 459–472
12. Rothery, R. A., and Weiner, J. H. (1991) *Biochemistry* **30,** 8296–8305
13. Trieber, C. A., Rothery, R. A., and Weiner, J. H. (1994) *J. Biol. Chem.* **269,** 7103–7109
14. Sambrook, J., Fritsch, E. F., and Maniatis, T. (1989) *Molecular Cloning: A Laboratory Manual,* 2nd Ed., Cold Spring Harbor Laboratory, Cold Spring Harbor, NY
15. Bilous, P. T., and Weiner, J. H. (1985) *J. Bacteriol.* **162,** 1151–1155
16. Weiner, J. H., MacIssac, D. P., Bishop, R. E., and Bilous, P. T. (1988) *J. Bacteriol.* **170,** 1505–1510
17. Markwell, M. A. D., Haas, S. M., Bieber, L. L., and Tolbert, N. E. (1978) *Anal. Biochem.* **87,** 206–210
18. Paulsen, K. E., Stankovich, M. T., and Orville, A. M. (1993) *Methods Enzymol.* **227,** 396–411
19. Cammack, R., and Weiner, J. H. (1990) *Biochemistry* **29,** 8410–8416
20. Cornforth, J. W., and James, A. T. (1956) *Biochem. J.* **63,** 124–130
21. Halford, S. E. (1975) *Biochem. J.* **149,** 411–422
22. Hiromi, K. (1979) *Kinetics of Fast Enzyme Reactions*, pp. 187–286, Halsted Press, New York
23. Hammes, G. G. (1982) *Enzyme Catalysis and Regulation*, pp. 61–75, Academic Press, New York
24. Giordani, R., Buc, J., Cornish-Bowden, A., and Cardenas, M. L. (1997) *Eur. J. Biochem.* **250,** 567–577
25. Shiraishi, F., and Savageau, M. A. (1992) *J. Biol. Chem.* **267,** 22934–22943
26. Kotik, M., and Zuber, H. (1992) *Biochemistry* **31,** 7787–7795
27. Jackson, G. S., Staniforth, R. A., Halsall, D. J., Atkinson T., Holbrook, J. J., Clarke, A. R., and Burston, S. G. (1993) *Biochemistry* **32,** 2554–2563
28. Holland, L. Z., McFall-Ngai, M., and Somero, G. N. (1997) *Biochemistry* **36,** 3207–3215
29. Van Hellemond, J. J., Klockiewicz, M., Gaasenbeek, C. P., Roos, M. H., and Tielens, A. G. (1995) *J. Biol. Chem.* **270,** 31065–31070
30. Buc, J., Santini, G. L., Blasco, F., Giordani, R., Cardenas, M. L. Chippaux, M. L. Cornish-Bowden, A., and Giordano, G.(1995) *Eur. J. Biochem.* **234,** 766–772
31. Magalon, A., Rothery, R. A., Lemesle-Meunier, D., Frixon, C., Weiner, J. H., and Blasco, F. (1998) *J. Biol. Chem.* **273,** 10851–10856
32. Roy, C., Lancaster, D., and Michel, H. (1997) *Structure* (*Lond.*) **5,** 1339–1359
33. Xia, D., Yu, C.-A., Kim, H., Xia, J.-Z., Kachurin, A. M., Zhang, L., Yu, L., and Deisenhofer, J. (1997) *Science* **277,** 60–66
34. Rothery, R. A., and Weiner, J. H. (1998) *Eur. J. Biochem.* **254,** 588–595